

^{99m}Tc -exorphin C: A new peptide radiopharmaceutical for tumor imagingT. Ertay,^{1*} P. Unak,² C. Tasci,¹ F. Z. Biber,¹ F. Zihnioglu,³ H. Durak¹¹ Dokuz Eylül University, Medical School, Dept. of Nuclear Medicine, Inciraltı, Turkey² Ege University, Institute of Nuclear Sciences, Dept. of Nuclear Applications, Bornova, Turkey³ Ege University, Faculty of Sciences, Department of Biochemistry, Bornova, Izmir, Turkey

(Received December 28, 2004)

The aim of this study was to label exorphin C with ^{99m}Tc and to examine its usefulness as opioid receptor binding radiopharmaceutical in Albino Wistar rats. Exorphin C, which is a peptide with 5 aminoacids, was labeled with ^{99m}Tc using glucoheptonate (GH) as a bifunctional chelating agent. Labeling efficiency was higher than 98%. The compound was stable for at least 5 hours at room temperature. Mammary tumor bearing Albino Wistar rats were imaged using gamma-camera. Biodistribution studies were also performed. Results demonstrated that ^{99m}Tc -glucoheptonate-exorphin C (^{99m}Tc -GE) analogs may be useful as a new class of receptor-binding peptides for the diagnosis and therapy of some cancer diseases related with opioid receptor-expressing tissues.

Introduction

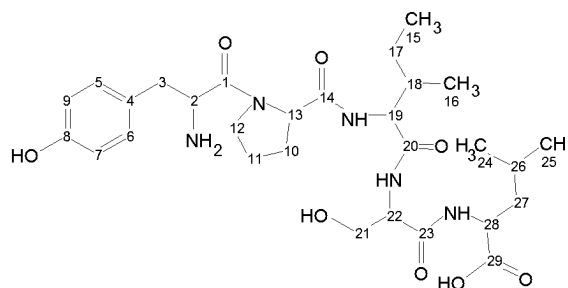
Peptides are known as receptor specific molecules which play an important role not only in the diagnosis and therapy of neoplastic diseases, but also in the pathogenesis of other diseases. The receptor specificity of peptides has, therefore, generated excitement in the field of nuclear medicine and hopes are high that investigations will lead to the development of many clinically useful radiopharmaceuticals.^{1–3} The successful use of ^{111}In -DTPA-Octreotide (Octreoscan) in the diagnosis of somatostatin receptor positive tumors has intensified the search for new target specific radiopharmaceuticals based on peptides. Many small peptides have been synthesized, radiolabeled, and studied for their potential use as new diagnostic imaging agents. Peptides have been labeled with various radionuclides such as ^{131}I , ^{123}I , ^{125}I , ^{111}In , ^{99m}Tc , ^{90}Y , ^{67}Ga , ^{64}Cu , ^{18}F and ^{186}Re using different methods.^{3–12} A number of human tumor tissues overexpress certain types of high affinity receptors on their cell-surface which can be used as targets for the in vivo imaging and therapy. The finding of new tumor localizing radiopharmaceuticals is an important challenge in the field of cancer research.^{13–15}

Exorphin C is a peptide with 5 amino acids (Tyr-Pro-Ile-Ser-Leu). It has an affinity to opioid receptor expressing tissues and tumors.¹⁶ FUKUDOME et al.^{17,18} isolated gluten exorphin C (Scheme 1) from the digest which is hydrolyzed with only gastro-intestinal proteases, pepsin, trypsin and chymotrypsin. This means that this peptide is released in digestive organs after the ingestion of wheat gluten. It has been reported that the oral administration of the peptic digest of wheat gluten influenced the regulation of gastro-intestinal motility and hormone release, and these effects have been

reversed by naloxone. In this respect, it might be possible that gluten exorphin C is responsible for such a regulation of physiological functions.^{17,18} The aim of this study was to label exorphin C with ^{99m}Tc using GH as chelating agent and to investigate its radiopharmaceutical potential on mammary tumor bearing Albino Wistar rats.

Experimental*Labeling procedure of exorphin C with ^{99m}Tc*

Ten mg of GH (Sigma Chemical Co.) was dissolved in 1 ml distilled water, 300 μg (in 0.5 ml water) stannous chloride and 259 MBq of $^{99m}\text{TcO}_4^-$ (in 0.5 ml), 300 ng (in 0.5 ml) exorphin C [Tyr-Pro-Ile-Ser-Leu] trifluoroacetate salt (Sigma Chemical Co.), were added to the solution and then the mixture was heated for 10 minutes at 90 °C. After cooling to room temperature, quality controls were performed by ITLC, paper electrophoresis and HPLC.



Scheme 1. Molecular structure of exorphin C

* E-mail: turkan.ertay@deu.edu.tr

Quality control procedures

ITLC: For ITLC, acetone, phosphate and physiological serum solutions and ITLC-SG sheets (Biodex, $0.5 \times 5 \text{ cm}^2$) were used as mobile and as static phases, respectively. Radiochromatograms were obtained using a radioscaner (Biodex Atommaster Radiochromatography, Model 149-201).

R_f values were also found using ITLC-SG sheets ($1 \times 10 \text{ cm}^2$) as static phases and acetone, phosphate and physiological serum as mobile phases. The sheets were cut into 1 cm pieces and counted by a counting system [Biodex (Atomlab 900) $2'' \times 2''$ NaI(Tl)]. R_f values were obtained from these counts.

Paper electrophoresis: Paper electrophoresis was performed using Whatman No. 1 cellulose acetate sheets ($1.5 \times 25 \text{ cm}^2$) and 0.1M phosphate buffer solution (pH 7.2). Applied voltage was 300 V for 2 hours. Developed strips were dried and cut into 1 cm pieces. They were counted by Cd(Te) detector equipped gamma-counter. Electrophoresis diagrams were obtained from these counts.

HPLC: Analyses of labeled peptide was accomplished by reversed phase low pressure gradient HPLC (Shimadzu LC-10 ATVP) on an ODS column (C_{18} - $4.6 \times 250 \text{ mm}^2$, Macharey-Nagel Inc). Ten μl (1.43 ng) of sample was applied to the column and eluted with linear gradient between 90% to 10% acetonitrile/phosphate at 0.8 ml/min. Column oven was set at 50°C . The elution was monitored at 210 and 255 nm UV and Cd(Te) radioactivity detectors.

Lipophilicity: Lipophilicity was determined for ^{99m}Tc -GH-exorphin-C (^{99m}Tc -GE) and compared with theory using the ACD (Additive Consecutive Algorithm) program. We used 3 different solutions (water, phosphate and physiological serum) and n-octanol to estimate the lipophilicity of ^{99m}Tc -GE for each one solution under the same conditions. Five hundreds μl of potassium phosphate (pH 7.4), 500 μl of n-octanol, and 1 μCi of labeled molecule were added to the glass tube and the mixture was vigorously shaken in a vortex mixer for long enough to reach equilibrium. After equilibration for a few minutes, the mixture was centrifuged 10 minutes at 4000 rpm to achieve good separation. The same procedure was applied to the other solutions. The two separated phases were added to the other tubes and the activity measured. The lipophilicity was calculated using the formula

$$\log P = A_0/A_w$$

Calculated values were compared with theoretical lipophilicity values obtained from the ACD computer program.

Biodistribution and scintigraphic imaging

Biodistribution on rats: The protocol was approved by the Institutional Animal Review Committee of Ege University. Tissue distribution studies were performed administering 3.7 MBq of ^{99m}Tc -GE to the rats which were 24 weeks age and with a weight range of 150–200 g by tail vein. Three rats were used per group at each time point. Rats were sacrificed at different time points (10, 30, 120 and 240 minutes) under intense ether anesthesia, organs were removed and counted. Time-activity curves were generated (Fig. 4). For receptor saturation studies, 1 μg exorphin C (in 0.3 ml serum physiological) was administered to the rats 15 minutes before the ^{99m}Tc -GE injection (Fig. 5). The above procedure was repeated for biodistribution of receptor saturated rats.

Imaging on control and mammary tumor bearing rats: Breast tumors were induced in female Albino Wistar rats at 53 days of age and 50–65 g weight by oral administration of 7.5 mg of 7,12-dimethylbenzanthracene (DMBA) in 0.4 ml corn oil emulsion. The rats were housed on a regular 12:12 light/dark cycle. After 3 months, DMBA administration was repeated with oral administration of 18 mg of DMBA in 0.9 ml corn oil (100–110 g weight). After 2 months from the second administration of DMBA, breast tumors appeared and the rats were then subjected to the experiment within 5 months. The rats were imaged from anterior projection using the gamma camera (Camstar XR/T, General Electric) equipped with a low energy general purpose collimator at 1, 10, 30, 60, 120, 300 and 1440 minutes. For quantitative evaluation, regions of interest were drawn on organs, tumor site and time-activity curves were generated.

Statistical analyses

Differences in the mean values of measured activities were evaluated statistically by Univariate Analysis of Variance of SPSS 10 computer program. Two tailed Pearson correlation was applied. The level of significance was considered below 0.05.

Results

The labeling efficiency was $98.7 \pm 0.3\%$ ($n = 12$). The labeled complex was stable for at least 5 hours at room temperature. Figures 1 to 3 show ITLC diagrams of ^{99m}Tc -GE. R_f values of the relevant ^{99m}Tc complexes are represented in Table 1. Electrophoresis diagrams show that the labeled product has anionic structure (Fig. 4). Charge affects general biodistribution, pharmacokinetics, metabolism and excretion characteristics as well as tissue uptake kinetics.

For conjugation of peptides to bifunctional chelates, the N terminus of peptide covalently links to the carboxyl group of the bifunctional chelate and an amide bond occurs between peptide and bifunctional chelate. Therefore, ^{99m}Tc-GE has an anionic structure as expected.

Table 1. *R_f* values of relevant complexes

Compound	Physiological serum (<i>R_f</i>)	Acetone (<i>R_f</i>)	Phosphate buffer
Na ^{99m} TcO ₄	1	1	1
^{99m} TcO ₂	0	0	0
^{99m} Tc-GH	0.4	0	0.6
^{99m} Tc-GE	0.9	0	0.9

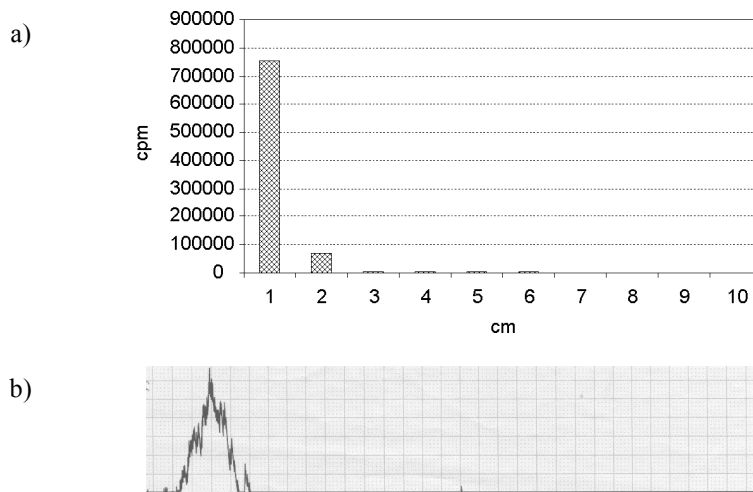


Fig. 1. ITLC-SG in acetone (a); radioscan in acetone (b)

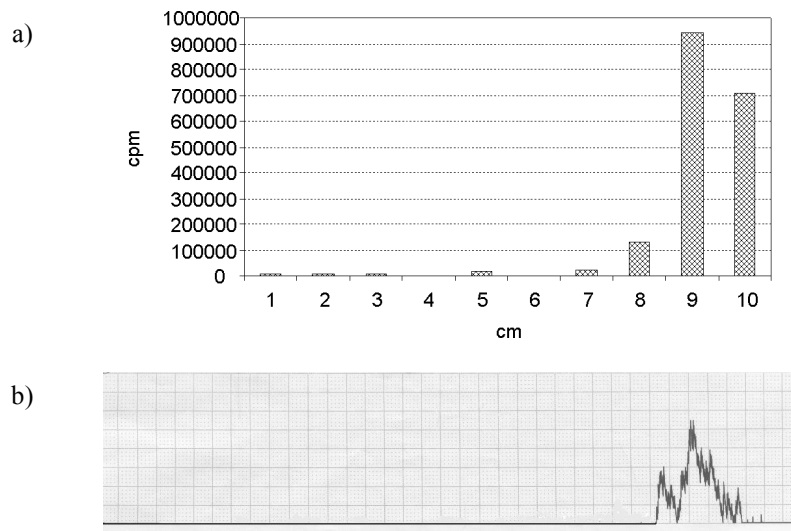


Fig. 2. ITLC-SG in physiological serum (a); radioscan in physiological serum (b)

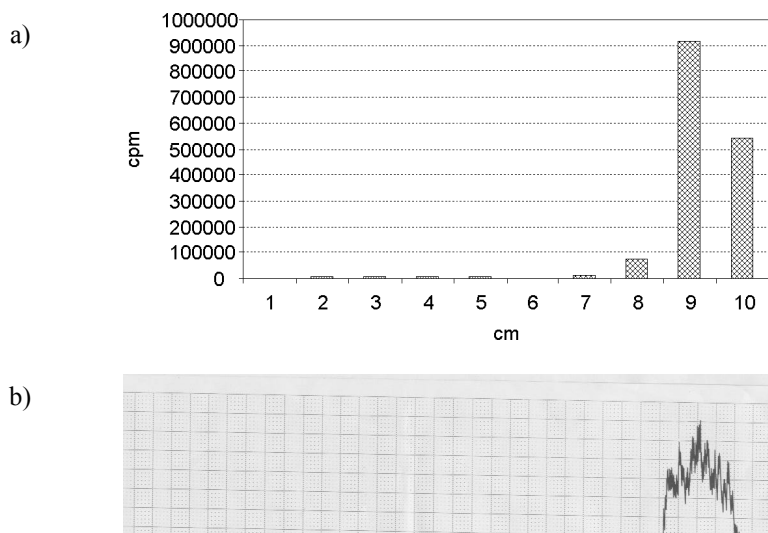


Fig. 3. ITLC-SG in phosphate buffer (a); radioscans in phosphate buffer (b)

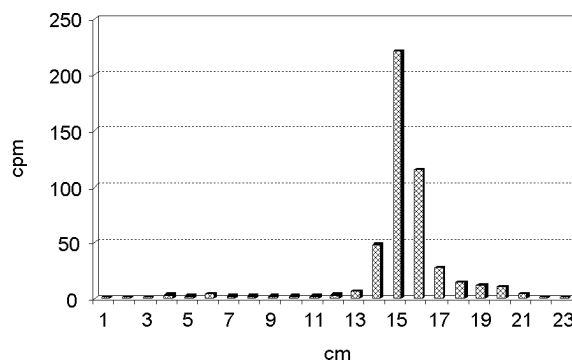


Fig. 4. Electrophoresis diagram in phosphate buffer

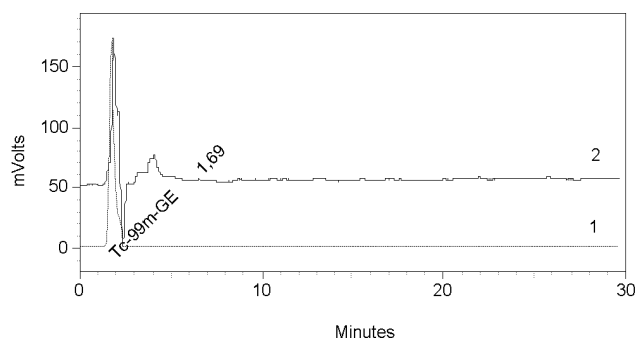


Fig. 5. HPLC chromatograms in radioactivity detector (1) and UV detector (2)

HPLC chromatograms were recorded with both UV and Cd(Te) detectors at the same time point (Fig. 5). This confirms that the ^{99m}Tc was attached to the peptide molecule in high efficiency.

For the biological transport properties of peptides, $\log P_{o/w}$ is sometimes a good indicator. The logarithm of the partition coefficient between n-octanol and water or

phosphate ($\log P_{o/w}$) is an important parameter widely used to characterize molecular lipophilicity and hydrophobicity.¹⁹ Lower lipophilicity leads to renal excretion. $\log P_{o/w}$ was found to be -1.14 ± 0.1 for ^{99m}Tc -GE while the theoretical value was 1.23 according to Additive Consecutive Algorithm (ACD) program (Table 2).

Table 2. Activity ratios of tumor to organs for ^{99m}Tc -Ge and ^{111}In labeled somatostatin analogs at the 4th hours

4th hours	Tumor/kidney	Tumor/liver	Tumor/muscle
^{111}In DOTAOC	0.96	4.4	69
^{111}In DOTAVAP	0.35	2.5	22.5
^{111}In DOTALAN	0.33	5.28	38
^{111}In Octreoscan	0.13	3.99	27.5
^{99m}Tc -GE	0.26	1.48	6.18

Biodistribution of ^{99m}Tc -GE in rat is shown in Fig. 6. Approximately 0.23% uptake for uterus and 0.14% uptake for ovaries appeared in the first minutes postinjection. Afterwards, while blood activity decreased, heart, kidneys and large intestines exhibited some activity since main excretion way was renal. However, small amounts of hepatobiliary excretion were also seen. There was no significant uptake in lungs, liver, spleen and pancreas.

Figure 7 represents biodistribution of ^{99m}Tc -GE in rat after saturation of opioid receptors with cold ligand. Activities in ovaries and uterus were decreased after

receptor saturation. However, activities in stomach and intestines were increased after 60-minute postinjection. Stomach/blood ratio was increased to 150 after 60-minute post injection with receptor saturation. This ratio was increased to 240 in large intestines after 240-minute post injection with receptor saturation. It may be speculated that the reason may be some enzymatic activities in gastrointestinal system after administration of cold ligand. Kidneys, uterus and ovaries to blood ratios were also increased with receptor saturation.

In imaging studies of tumor bearing rats, there was constant activity in the region of tumor until the end of the study. The scintigraphic image of a tumor bearing rat is seen in Fig. 8. Tumor/background values were obtained from ROI (region of interest) on a tumor bearing rat (Fig. 9). Activity uptake was seen in tumor after the first minute postinjection and significant uptake was still subsisted up to 24 hours. Removing the tumor and organs studied, the activity on tumor tissue was thirty times higher than muscle (background).

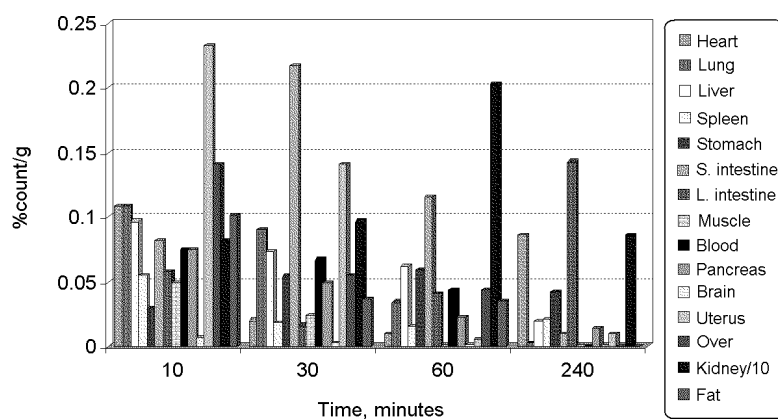


Fig. 6. Biodistribution of ^{99m}Tc -GE in rat

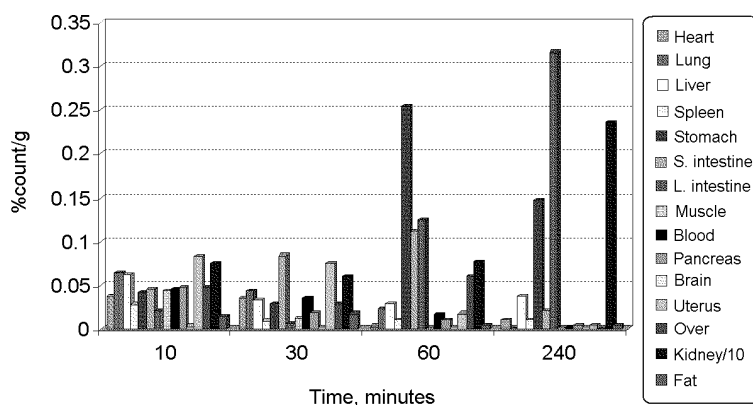


Fig. 7. Biodistribution of ^{99m}Tc -GE in rat after saturation of opioid receptors with cold ligand

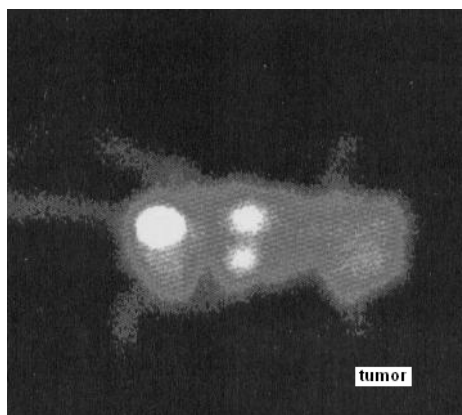


Fig. 8. Image of ^{99m}Tc -GE on tumor bearing rat

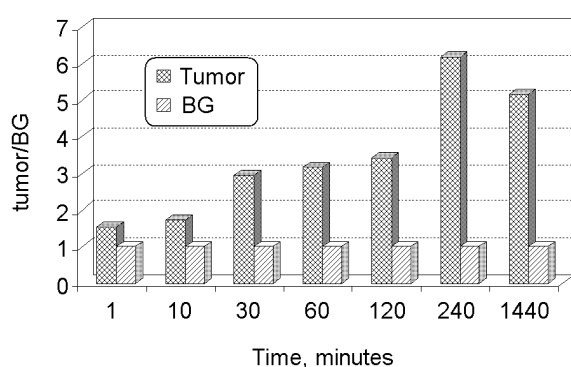


Fig. 9. Time-activity curve (tumor/BG) on tumor bearing rat by ROI

Table 3. Activity ratios of tumor to organs for ^{99m}Tc -GE at the 24th hours

24th hours	Tumor/kidney	Tumor/liver	Tumor/muscle
^{99m}Tc -GE	9.07	11.81	32.30

Discussion

Peptides play an important role as regulators of growth and other cellular functions in normal but also in tumor tissues. Many tumors overexpress receptors for regulatory peptides and many of these receptors mediate growth regulating effects *in vitro*. Certain types of tumors also respond to the growth inhibiting or growth promoting signals of peptides *in vivo*, an effect which has become an important clinical approach to treatment of tumors in man. When labeled with gamma-emitting radionuclides, opioid-peptides have the potential to localize opioid-receptor-positive tumors using gamma camera scintigraphy.^{12,13}

Renal excretion was observed which is the characteristic of small peptides.²⁰ Moreover, the radiopeptide is rapidly cleared via the urinary system

showing much lower liver uptake and a more favorable biodistribution. With receptor saturation hepatobiliary excretion was decreased.

In the imaging study of tumor bearing rat, the tumor was clearly visualized from the first minute postinjection. The specificity of ligand binding *in vivo* was demonstrated by the high tumor/non-tumor ratio at 4 hours postinjection. There was constant activity in the tumor region until the end of the study. We can speculate that ^{99m}Tc -GE can be successfully used to detect opioid receptor positive tumor tissues (SCLC, neuroblastoma and breast). This radiopeptide was compared to somatostatin analogs labeled with ^{111}In in tumor tissues (Table 2).¹³ Although tumor/kidney ratio was only slightly higher than ^{111}In Octreoscan, tumor/liver and tumor/muscle ratios are lower than other ^{111}In labeled peptides such as ^{111}In DOTAOC, ^{111}In DOTAVAP, ^{111}In DOTALAN in the 4th hours. However, we found significantly higher tumor/organ ratios in 24th hours (Table 3). Because of favorable nuclear physical characteristics and ready availability of ^{99m}Tc , ^{99m}Tc -GE may be an alternative imaging for tumor tissue.

Although considerable activity was seen in the rabbit brain, there was no considerable uptake in the rat brain. ^{99m}Tc -GE was not able to cross the rat blood brain barrier according to our previous results.²¹

Conclusions

In conclusion, the labeling efficiency was high and stability was adequate for imaging.

Results demonstrated that ^{99m}Tc -GE analogs may be useful as a new class of receptor-binding peptides for the diagnosis and perhaps therapy of some cancer diseases related with opioid receptor-expressing tissues. Results of this study are sufficiently encouraging to bring about further evaluation of these and related compounds as possible opioid based tumor imaging agents.

*

Parts of the study were presented in 2004 at the 6th International Congress of Nuclear Oncology, Çeşme, Turkey. The authors thank for the financial supports of the Ege University Scientific Research Fund.

References

1. S. ADAMS, R. BAUM, T. RINK, P. M. SCHUMM-DRÄGER, K. H. USADEL, G. HÖR, *Eur. J. Nucl. Med.*, 25 (1998) 79.
2. T. M. BEHR, M. GOTTHARDT, A. BARTH, M. BEHE, *J. Nucl. Med.*, 45 (2001) 189.
3. A. J. FISCHMAN, J. W. BABICH, W. H. STRAUSS, *J. Nucl. Med.*, 34 (1993) 2253.
4. C. J. ANDERSON, T. S. PEJEAU, B. W. EDWARDS, E. L. C. SHERMAN, B. E. ROGERS, M. J. WELCH, *J. Nucl. Med.*, 36 (1995) 2315.

5. T. M. BEHR, N. JENNER, M. BEHE, C. ANGERSTEIN, S. GRATZ, F. RAUE, W. BECKER, *J. Nucl. Med.*, 40 (1999) 1029.
6. W. A. BREEMAN, L. J. HOFLAND, M. VAN DER PLUJIM, P. M. KOETSVELD, M. JONG, B. SETYONO-HAN, W. H. BAKKER, D. J. KWEKKEBOOM, T. J. VISSER, S. W. J. LAMBERTS, E. P. KRENNIG, *Eur. J. Nucl. Med.*, 21 (1994) 328.
7. M. K. DEWANJEE, *Sem. Nucl. Med.*, 20 (1990) 5.
8. T. ERTAY, P. UNAK, R. BEKIS, F. YURT, F. Z. BIBER, H. DURAK, *Nucl. Med. Biol.*, 28 (2001) 194.
9. M. JONG, W. H. BAKKER, E. P. KRENNIG, W. A. P. BREEMAN, M. E. PLUJIM, B. F. BERNARD, T. J. VISSER, E. JERMAN, M. BEHE, P. POWELL, H. R. MACKE, *Eur. J. Nucl. Med.*, 24 (1997) 368.
10. S. J. MATHER, *Modern Trends in Radiopharmaceuticals for Diagnosis and Therapy*, IAEA-TECDOC-1029, Portugal, 30 March–3 April 1998, p. 19.
11. D. A. PEARSON, J. LISTER-JAMES, W. J. MCBRIDE, D. M. WILSON, L. J. MARTEL, E. R. CIVITELLO, J. E. TAYLOR, B. R. MOYER, R. T. DEAN, *J. Med. Chem.*, 39 (1996) 1361.
12. M. L. THAKUR, V. R. PALLELLA, *Modern Trends in Radiopharmaceuticals for Diagnosis and Therapy*, IAEA-TECDOC-1029, Portugal, 30 March–3 April 1998, p. 63.
13. A. HEPPELER, S. FROIDEVAUX, A. N. EBERLE, H. R. MAECKE, *Curr. Med. Chem.*, 7 (2000) 971.
14. J. C. REUBI, *J. Nucl. Med.*, 36 (1995) 1846.
15. I. VIRGOLINI, Q. YANG, S. LI, P. ANGELBERGER, N. NEUHOLD, B. NIEDERLE, *Cancer Res.*, 54 (1994) 690.
16. S. FUKUDOME, Y. JINSMAA, T. MATSUKAWA, R. SASAKI, M. YOSHIKAWA, *FEBS Lett.*, 412 (1997) 475.
17. S. FUKUDOME, M. YOSHIKAWA, *FEBS Lett.*, 296 (1992) 107.
18. S. FUKUDOME, M. YOSHIKAWA, *FEBS Lett.*, 316 (1993) 17.
19. P. BUCHWALD, N. BODOR, *Protein: Structure, Function Genetics*, 30 (1998) 80.
20. J. LISTER-JAMES, B. R. MOYER, T. DEAN, *QC Nucl. Med.*, 40 (1996) 221.
21. T. ERTAY, P. UNAK, C. TASCI, F. ZIHNIOGLU, H. DURAK, *Appl. Radiation Isotopes*, (2005) in press.